Dynamics of the Wet-end Section in Paper Mills

Yeong-Koo Yeo†, Jae Young Ryu and Sung Chul Yi

Department of Chemical Engineering, Hanyang University, Seoul 133-791, Korea
(*Received 13 August 2004 • accepted 26 October 2004*)

Abstract−A model representing the wet-end section of a paper mill has been developed to characterize its dynamic behavior during the grade change. The model is based on the mass balance relationships written for the simplified wet-end white water network. From the linearization of the dynamic model, higher-order Laplace transfer functions were obtained followed by the reduction procedure to give simple lower-order models in the form of 1st-order or 2nd-order plus dead times. The dynamic response of the wet-end is influenced both by the white water volume and by the level of wire retention. Effects of key manipulated variables such as the thick stock flow rate, the ash flow rate and the retention aid flow rate on the major controlled variables were analyzed by numerical simulations. The simple dynamic model developed in the present study can be effectively used in the operation and control.

Key words: Bone-dry Weight, Consistency, Dynamic Model, Paper Mill, Retention, Linearization, Wet-end

INTRODUCTION

The formation of a sheet of paper is a continuous process in which cellulose fibers, fines, fillers and additives form a network that is then pressed and dried. The three-dimensional network is formed by the mechanical entanglement of the fibers and by the chemical interactions between the different pulp fractions. The complexity of the wet-end system of a paper mill is not readily apparent. The increased stringent environmental demands on paper production have led to the use of more closed wet-end systems with considerable material recirculation. It is possible to operate a paper machine successfully without a detailed understanding of how the changes in one part of the system will affect the other parts of the system. But, when operational troubles arise, it is necessary to interpret plant data correctly and to cross check the normal operating conditions of the plant. It is helpful to have current information on a particular system at hand when required, rather than to rely on spot sampled data with relatively low reliability. A dynamic model can be a powerful tool to provide reliable data for a particular section being considered. Apart from the process control and trouble-shooting for the wet-end section, the dynamic model can be an essential tool in the design of new systems and in the modification of existing systems [Yeo et al., 2003], as well as in the analysis of process variables and in the identification of the effect of various additives on the dynamic behavior of the system.

Simple white water material balances for the wet-end system were proposed to compute equilibrium concentrations of solid components [Mardon and Serenius, 1971; Yeo et al., 2004]. A simple model of this kind can be used to check the abnormality of the present operational status. With rapid development and application of various computer operation-aid systems, the operation of the plant is monitored and controlled on-line and the steady-state model can find

its use only in very restricted area. Investigations on dynamics of the short circulation system with constant retentions were reported [Norman, 1990]. During the operation, retention changes due to machine speed changes, basis weight changes and retention aid changes. Retention changes have great effect on basis weight and ash percentage controls. However, there is no physically based dynamic model to predict the behavior of key controlled variables for given operating conditions. A dynamic model is especially useful to investigate the dynamic behavior of the wet-end system during the grade change. Use of a simple plant-wide dynamic model in the transition control during a grade change was proposed [Murphy and Chen, 1999; Skoglund and Brundin, 2000; Vhtamaki, 2001]. Application of model predictive control schemes based on the transfer function dynamic models was also reported [Hauge and Lie, 2002].

The objective of the present work is to develop a simple dynamic model for a wet-end section to analyze the transient behavior of the white water network during the grade change. From the linearization of the dynamic model, Laplace transfer functions representing the effects of key variables were developed. This kind of model for the paper mill has been reported before [Berrada et al., 1997]. The high-order (normally more than 4th or 5th order) transfer functions initially obtained from the linearization are not adequate in the model predictive control operations [Chyi and Chuang, 1994]. There are many benefits of simplified dynamic models such as less computational time, easier analysis and interpretation and convenient controller design. The model gives the bone-dry weight of the paper and dynamics of the retention for specific grade change operating conditions.

MODELING OF WET-END SECTION

1. Short Circulation

Historically, the water and fiber flow system in a paper and board mill was simple and straightforward. Fresh water was used for diluting the raw material to a stock, with a consistency suitable for preparation. The stock was subsequently diluted to a mix, with a consistency low enough for forming, again using fresh water. There

---

†To whom correspondence should be addressed.
E-mail: ykyeo@hanyang.ac.kr
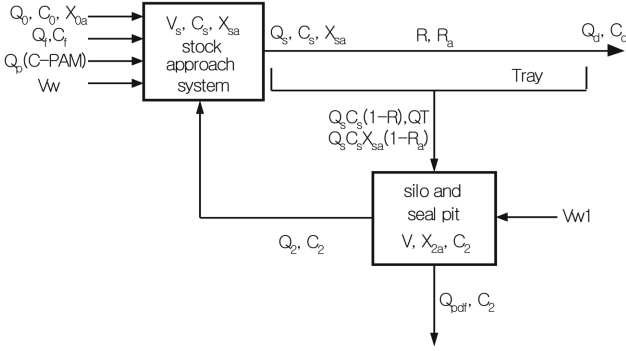‡This paper is dedicated to Professor Se Ki Moon on the occasion of his retirement from Hanyang University.

Fig. 1. Schematic of wet-end section.

was no recirculation of either water or fiber. But, due to shortage of fresh water supplies, to economic incentive for recovery of material from the waste water and lately also to environmental reasons, recirculation of water and material within the process has been introduced, and white water system of modern paper machines is relatively closed and generally very complex.

Fig. 1 shows a simplified wet-end system of a paper plant. In Fig. 1, the thick stock rate Q_0, the ash flow rate Q_f, the ash fraction of the thick stock X_{0a} and the flow rate of the retention aid Q_p are assumed to be known, i.e., they are manipulated variables. These variables become input data for the model to be developed.

First we define a parameter p_1 as

$$p_1 = 1000kP_wS_wJ_rC_F \qquad (1)$$

where S_w and P_w are the width of the slice and the pond, respectively, and C_F is the headbox slice factor which is dependent upon the configuration of the outlet device of the headbox. The product $P_wS_wC_F$ gives the area of the headbox outlet section. J_r represents the jet/wire ratio, which is defined as the ratio of the flow rate from the headbox to the wire speed. In normal operations, J_r is slightly greater than 1. Due to the draw in the drying section, the paper web moves faster in the reel section than in the wire. The factor k represents the difference in the speed between the wire section and the reel part. In most operations the speed in the wire section is 97% of the speed in the reel section. This means that we can set the value of k as 0.97 in most cases. The flow rate from the headbox Q_s is given by

$$Q_s = p_1V_r \qquad (2)$$

where V_r is the reel speed. Q_s is the jet flow rate form the slice taking into account of the effect of Vena contractor. The flow rate to the press is then expressed as

$$Q_d = \frac{p_1V_rC_sR}{C_d} \qquad (3)$$

where R is the retention ratio, C_s is the consistency in the headbox and C_d is the consistency of the stream to the press. C_d lies in the range of 18-22% and is set to 20% in the simulations. The product $p_1V_rC_s$ is the amount of the mass from the headbox. From the simple material balance around the wire and the tray, the flow rate Q_T of the stream to the silo and the seal pit is given by

$$Q_T = Q_s - Q_d = p_1V_r - \frac{p_1V_rC_sR}{C_d} \qquad (4)$$

In an actual operation, the amount of supplementary water cannot be neglected. Thus we introduce V_{w1} to take into account the amount of supplementary water. The flow rate of the stream to save-all Q_{pdf} can be obtained from the material balance around the wire, the silo and the seal pit and can be expressed as

$$Q_{pdf} = p_2V_r - p_2V_rC_sR + V_{w1} - (p_1V_r - Q_0 - Q_f - Q_p - V_w) \qquad (5)$$

where p_2 is given by

$$p_2 = \frac{p_1}{C_d}$$

Q_2 is the flow rate of the internal circulation stream and is given by

$$Q_2 = p_1V_r - Q_0 - Q_f - Q_p - V_w \qquad (6)$$

where V_w is the amount of dilution water. Perfect mixing in all the components (Fig. 1) with significant volume is assumed in this simplified model.

2. Modeling of Silo and Stock Approach

Dynamics of the solid and ash contents in the silo and the seal pit can be expressed as

$$\frac{dC_2}{dt} = \frac{1}{V}\{(1-R)p_1V_rC_s - Q_2C_2 + C_2(p_1V_r - p_2V_rC_sR + V_{w1} - Q_2)\} \qquad (7)$$

$$\frac{dX_{2a}}{dt} = \frac{1}{VC_2}[(1-R_a)P_1V_rC_sX_{sa} - Q_2C_2X_{2a} - \cdots - C_2X_{2a}(p_1V_r - p_2V_rC_sR + V_{w1} - Q_2)] - \frac{X_{2a}}{C_2}\frac{dC_2}{dt} \qquad (8)$$

where C_2 is the silo consistency, X_{2a} is the ash fraction in the silo and R_a is the ash retention. V denotes the total volume of the silo and the sealpit. Similarly, dynamics in the stock approach section are given by

$$\frac{dC_s}{dt} = \frac{1}{V_s}\{Q_0C_s + C_2(p_1V_r - Q_0 - Q_f - Q_p - V_w) + Q_fC_f - p_1V_rC_s\} \qquad (9)$$

$$\frac{dX_{sa}}{dt} = \frac{1}{V_sC_s}\{Q_0C_0X_{0a} + C_2X_{2a}(p_1V_r - Q_0 - Q_f - Q_p - V_w) + Q_fC_f - p_1V_rC_sX_{sa}\} - \frac{X_{sa}}{V_sC_s}\{Q_0C_s + C_2(p_1V_r - Q_0 - Q_f - Q_p - V_w) + Q_fC_f - p_1V_rC_s\} \qquad (10)$$

In this study, the stock approach section includes screens and cleaners as well as deculator. Because of the complexity of the configuration of cleaner sections and screens and of the considerable volume of the deculator, we supposed a tank with volume V_s to represent the stock approach section. We assumed that the flow from the tank becomes the outlet flow from the headbox. V_s includes the volume of the deculator, the volume of the 1st and 2nd cleaner lines and the volume of 1st and 2nd screen lines.

3. Retention and Bone Dry

Retention is affected by many factors such as the amount and types of retention aids, thick stock rates, types of pulp, SRE (specific refinery energy), fiber fine fraction in the thick stock, the wire speed, filler flow rates, temperature of the white water, PH, ash contents in the white water and the thick stock, and the wire mesh [Neimo, 2000]. In this work we are considering only the "short-term dynamics" during grade changes rather than the "long-term dynamics."

Then we can assume that retentions exhibit first-order dynamics and can represent the behavior of R and R_a as

$$\frac{dR}{dt} = \frac{k_1}{\tau}Q_p - \frac{R}{\tau} \tag{11}$$

$$\frac{dR_a}{dt} = \frac{k_2}{\tau}Q_p - \frac{R_a}{\tau} \tag{12}$$

where τ is the retention time constant, k_1 is the retention constant and k_2 is the ash retention constant. k_2 was assumed to be 1/3 of k_1. k_1 can be obtained from the steady-state retention and the amount of the retention aid. τ depends on the specific paper machine being used.

The bone dry weight BD and the ash bone dry ashBD are given by

$$BD = p_1 p_3 C_s R \tag{13}$$

$$ashBD = p_1 p_3 C_s X_{sa} R_a \tag{14}$$

$$p_3 = \frac{1000 C_w W_r}{P_w R_w} \tag{15}$$

where C_w and P_w are widths of the couch and the pond, respectively, and R_w is the reel width. W_r is the diminishment ratio of BD or ash BD which can occur unexpectedly while the paper web passes the press and dryer section.

TRANSFER FUNCTION MODELS

1. State-space Model

The reel speed, the thick stock flow, the filler flow, the retention aid flow, and the ash fraction of the thick stock serve as input variables in the model presented before (Eqs. (1)-(15)). The state variables are C_2, C_s, X_{2a}, X_{sa}, R and R_a. The two outputs are BD (bone dry weight) and ashBD (bone dry ash weight). The ash fraction of the thick stock was assumed to follow a ramp trajectory during the grade change operation. The linearized state equations are given by

$$\frac{dX}{dt} = AX + BU$$
$$Y = CX + DU \tag{16}$$

where

$$X = [C_2 X_{2a} C_s X_{sa} R R_a]'$$
$$U = [V_r Q_0 Q_f Q_p X_{0a}]'$$
$$Y = [BD \; ashBD]'$$

Elements of the state-space system (16) are given by

$$\begin{pmatrix} C_2' \\ X_{2a}' \\ C_s' \\ X_{sa}' \\ R' \\ R_a' \end{pmatrix} = \begin{bmatrix} \frac{\partial C_2}{\partial C_2}\big|_s & \frac{\partial C_2}{\partial X_{2a}}\big|_s & \frac{\partial C_2}{\partial C_s}\big|_s & \frac{\partial C_2}{\partial X_{sa}}\big|_s & \frac{\partial C_2}{\partial R}\big|_s & \frac{\partial C_2}{\partial R_a}\big|_s \\ \frac{\partial X_{2a}}{\partial C_2}\big|_s & \frac{\partial X_{2a}}{\partial X_{2a}}\big|_s & \frac{\partial X_{2a}}{\partial C_s}\big|_s & \frac{\partial X_{2a}}{\partial X_{sa}}\big|_s & \frac{\partial X_{2a}}{\partial R}\big|_s & \frac{\partial X_{2a}}{\partial R_a}\big|_s \\ \frac{\partial C_s}{\partial C_2}\big|_s & \frac{\partial C_s}{\partial X_{2a}}\big|_s & \frac{\partial C_s}{\partial C_s}\big|_s & \frac{\partial C_s}{\partial X_{sa}}\big|_s & \frac{\partial C_s}{\partial R}\big|_s & \frac{\partial C_s}{\partial R_a}\big|_s \\ \frac{\partial X_{sa}}{\partial C_2}\big|_s & \frac{\partial X_{sa}}{\partial X_{2a}}\big|_s & \frac{\partial X_{sa}}{\partial C_s}\big|_s & \frac{\partial X_{sa}}{\partial X_{sa}}\big|_s & \frac{\partial X_{sa}}{\partial R}\big|_s & \frac{\partial X_{sa}}{\partial R_a}\big|_s \\ \frac{\partial R}{\partial C_2}\big|_s & \frac{\partial R}{\partial X_{2a}}\big|_s & \frac{\partial R}{\partial C_s}\big|_s & \frac{\partial R}{\partial X_{sa}}\big|_s & \frac{\partial R}{\partial R}\big|_s & \frac{\partial R}{\partial R_a}\big|_s \\ \frac{\partial R_a}{\partial C_2}\big|_s & \frac{\partial R_a}{\partial X_{2a}}\big|_s & \frac{\partial R_a}{\partial C_s}\big|_s & \frac{\partial R_a}{\partial X_{sa}}\big|_s & \frac{\partial R_a}{\partial R}\big|_s & \frac{\partial R_a}{\partial R_a}\big|_s \end{bmatrix} \begin{pmatrix} C_2' \\ X_{2a}' \\ C_s' \\ X_{sa}' \\ R' \\ R_a' \end{pmatrix}$$

$$+ \begin{pmatrix} \frac{\partial C_2}{\partial V_r}\big|_s & \frac{\partial C_2}{\partial Q_0}\big|_s & \frac{\partial C_2}{\partial Q_f}\big|_s & \frac{\partial C_2}{\partial Q_p}\big|_s & \frac{\partial C_2}{\partial X_{0a}}\big|_s \\ \frac{\partial X_{2a}}{\partial V_r}\big|_s & \frac{\partial X_{2a}}{\partial Q_0}\big|_s & \frac{\partial X_{2a}}{\partial Q_f}\big|_s & \frac{\partial X_{2a}}{\partial Q_p}\big|_s & \frac{\partial X_{2a}}{\partial X_{0a}}\big|_s \\ \frac{\partial C_s}{\partial V_r}\big|_s & \frac{\partial C_s}{\partial Q_0}\big|_s & \frac{\partial C_s}{\partial Q_f}\big|_s & \frac{\partial C_s}{\partial Q_p}\big|_s & \frac{\partial C_s}{\partial X_{0a}}\big|_s \\ \frac{\partial X_{sa}}{\partial V_r}\big|_s & \frac{\partial X_{sa}}{\partial Q_0}\big|_s & \frac{\partial X_{sa}}{\partial Q_f}\big|_s & \frac{\partial X_{sa}}{\partial Q_p}\big|_s & \frac{\partial X_{sa}}{\partial X_{0a}}\big|_s \\ \frac{\partial R}{\partial V_r}\big|_s & \frac{\partial R}{\partial Q_0}\big|_s & \frac{\partial R}{\partial Q_f}\big|_s & \frac{\partial R}{\partial Q_p}\big|_s & \frac{\partial R}{\partial X_{0a}}\big|_s \\ \frac{\partial R_a}{\partial V_r}\big|_s & \frac{\partial R_a}{\partial Q_0}\big|_s & \frac{\partial R_a}{\partial Q_f}\big|_s & \frac{\partial R_a}{\partial Q_p}\big|_s & \frac{\partial R_a}{\partial X_{0a}}\big|_s \end{pmatrix} \begin{pmatrix} V_{reel}' \\ Q_0' \\ Q_f' \\ Q_p' \\ X_{0a}' \end{pmatrix}$$

$$\begin{pmatrix} BD' \\ ashBD' \end{pmatrix} = \begin{pmatrix} \frac{\partial BD}{\partial C_2}\big|_s & \frac{\partial BD}{\partial X_{2a}}\big|_s & \frac{\partial BD}{\partial C_s}\big|_s & \frac{\partial BD}{\partial X_{sa}}\big|_s & \frac{\partial BD}{\partial R}\big|_s & \frac{\partial BD}{\partial R_a}\big|_s \\ \frac{\partial aB}{\partial C_2}\big|_s & \frac{\partial aB}{\partial X_{2a}}\big|_s & \frac{\partial aB}{\partial C_s}\big|_s & \frac{\partial aB}{\partial X_{sa}}\big|_s & \frac{\partial aB}{\partial R}\big|_s & \frac{\partial aB}{\partial R_a}\big|_s \end{pmatrix} \begin{pmatrix} C_2' \\ X_{2a}' \\ C_s' \\ X_{sa}' \\ R' \\ R_a' \end{pmatrix}$$

$$+ \begin{pmatrix} \frac{\partial BD}{\partial V_r}\big|_s & \frac{\partial BD}{\partial Q_0}\big|_s & \frac{\partial BD}{\partial Q_f}\big|_s & \frac{\partial BD}{\partial Q_p}\big|_s & \frac{\partial BD}{\partial X_{0a}}\big|_s \\ \frac{\partial aB}{\partial V_r}\big|_s & \frac{\partial aB}{\partial Q_0}\big|_s & \frac{\partial aB}{\partial Q_f}\big|_s & \frac{\partial aB}{\partial Q_p}\big|_s & \frac{\partial aB}{\partial X_{0a}}\big|_s \end{pmatrix} \begin{pmatrix} V_r' \\ Q_0' \\ Q_f' \\ Q_p' \\ X_{0a}' \end{pmatrix}$$

The elements of the coefficient matrices in the above relations can be evaluated from Esq. (7)-(14). Resulting state equations can be expressed as

$$\begin{pmatrix} C_2' \\ X_{2a}' \\ C_s' \\ X_{sa}' \\ R' \\ R_a' \end{pmatrix} = \begin{pmatrix} A_{11} A_{12} A_{13} A_{14} A_{15} A_{16} \\ A_{21} A_{22} A_{23} A_{24} A_{25} A_{26} \\ A_{31} A_{32} A_{33} A_{34} A_{35} A_{36} \\ A_{41} A_{42} A_{43} A_{44} A_{45} A_{46} \\ A_{51} A_{52} A_{53} A_{54} A_{55} A_{56} \\ A_{61} A_{62} A_{63} A_{64} A_{65} A_{66} \end{pmatrix} \begin{pmatrix} C_2' \\ X_{2a}' \\ C_s' \\ X_{sa}' \\ R' \\ R_a' \end{pmatrix}$$

$$+ \begin{pmatrix} B_{11} B_{12} B_{13} B_{14} B_{15} \\ B_{21} B_{22} B_{23} B_{24} B_{25} \\ B_{31} B_{32} B_{33} B_{34} B_{35} \\ B_{41} B_{42} B_{43} B_{44} B_{45} \\ B_{51} B_{52} B_{53} B_{54} B_{55} \\ B_{61} B_{62} B_{63} B_{64} B_{65} \end{pmatrix} \begin{pmatrix} V_{reel}' \\ Q_0' \\ Q_f' \\ Q_p' \\ X_{0a}' \end{pmatrix} \tag{17}$$

$$Y = CX + DU$$

In Eq. (17), the subscript s denotes the steady-state values. A_{ij} and B_{ij} in (17) and matrices C and D are given in Appendix.

2. Higher-order Transfer Functions

Initial higher-order Laplace transfer functions can be expressed in the form as given by

$$\begin{pmatrix} BD' \\ ashBD' \end{pmatrix} = \begin{pmatrix} G_{11}(s) G_{12}(s) G_{13}(s) G_{14}(s) G_{15}(s) \\ G_{21}(s) G_{22}(s) G_{23}(s) G_{24}(s) G_{25}(s) \end{pmatrix} \begin{pmatrix} V_r' \\ Q_0' \\ Q_f' \\ Q_p' \\ X_{0a}' \end{pmatrix} \tag{18}$$

where

$$G_{11} = \frac{-0.05514s - 0.02449}{s^2 + 1.849s + 0.4314} \tag{19}$$

$$G_{21} = \frac{-0.00584s^3 - 0.01532s^2 - 0.01113s - 0.003428}{s^4 + 4.035s^3 + 5.208s^2 + 2.303s + 0.3172} \tag{20}$$

$$G_{12} = \frac{0.005123s + 0.002654}{s^2 + 1.849s + 0.4314} \tag{21}$$

$$G_{22} = \frac{0.001507s^3 + 0.0003805s^2 + 0.0003251s + 0.000251}{s^4 + 4.035s^3 + 5.208s^2 + 2.303s + 0.3172} \tag{22}$$

$$G_{13} = \frac{0.07596s + 0.03448}{s^2 + 1.849s + 0.4314} \tag{23}$$

$$G_{23} = \frac{0.03988s^3 + 0.11s^2 + 0.08459s + 0.01779}{s^4 + 4.035s^3 + 5.208s^2 + 2.303s + 0.3172} \tag{24}$$

$$G_{14} = \frac{0.008795s^2 + 0.01705s - 0.001384}{s^3 + 1.856s^2 + 0.4437s + 0.002876} \tag{25}$$

$$G_{24} = \frac{\begin{array}{c}0.0006863s^5 + 0.0029s^4 + 0.003684s^3 \\ +0.0006853s^2 - 0.0008424s - 5.645e\text{-}006\end{array}}{\begin{array}{c}s^6 + 4.048s^5 + 5.262s^4 + 2.372s^3 \\ +0.3482s^2 + 0.004332s + 1.41e\text{-}005\end{array}} \tag{26}$$

$$G_{15} = 0 \tag{27}$$

$$G_{25} = \frac{29.29s + 26.99}{s^2 + 2.186s + 0.7353} \tag{28}$$

Pole-zero locations of these functions are shown in Fig. 2. There are no poles with positive real values and we can confirm that the wet-end system is stable. But $G_{14}(s)$ and $G_{24}(s)$ give positive zeros, which means that inverse responses are expected in BD and ashBD due to the change in the retention aid flow.

3. Reduction of the Transfer Functions

Higher-order transfer functions may cause numerical errors and increase computational load when they are used in the simulations or in the control operations such as the model predictive control. In fact, it is very difficult to formulate model predictive control problems by using higher-order transfer functions. Most chemical plants can be expressed by the transfer functions in the form of 1st-order plus dead time (FOPDT) or 2nd-order plus dead time (SOPDT). SOPDT is used to relate the input and the output characterized by inverse responses. In the identification of lower-order models, we first assume FOPDT or SOPDT models with unknown parameters. The higher-order model (18) serves as the actual plant. A simple pulse input as shown in Fig. 3 is introduced into the supposed models and the "plant" simultaneously and the resulting outputs are compared. Use of the PRBS (pseudo-random binary sequence) is the usual practice in this case. But a simple pulse function was found to be enough in the identification of the lower-order models. By minimization of the difference (29) between the supposed model output and the "plant" output, we can determine the best possible model parameters.

$$Q(F, Y) = \sum_{i=1}^{n} [F_i - Y_i]^2 \tag{29}$$

where i is the sampling number, F_i is the output from the higher-order model and Y_i is the output computed from the assumed FOPDT or SOPDT model. Various optimization algorithms can be used in the minimization, but the simple least-squares method was enough
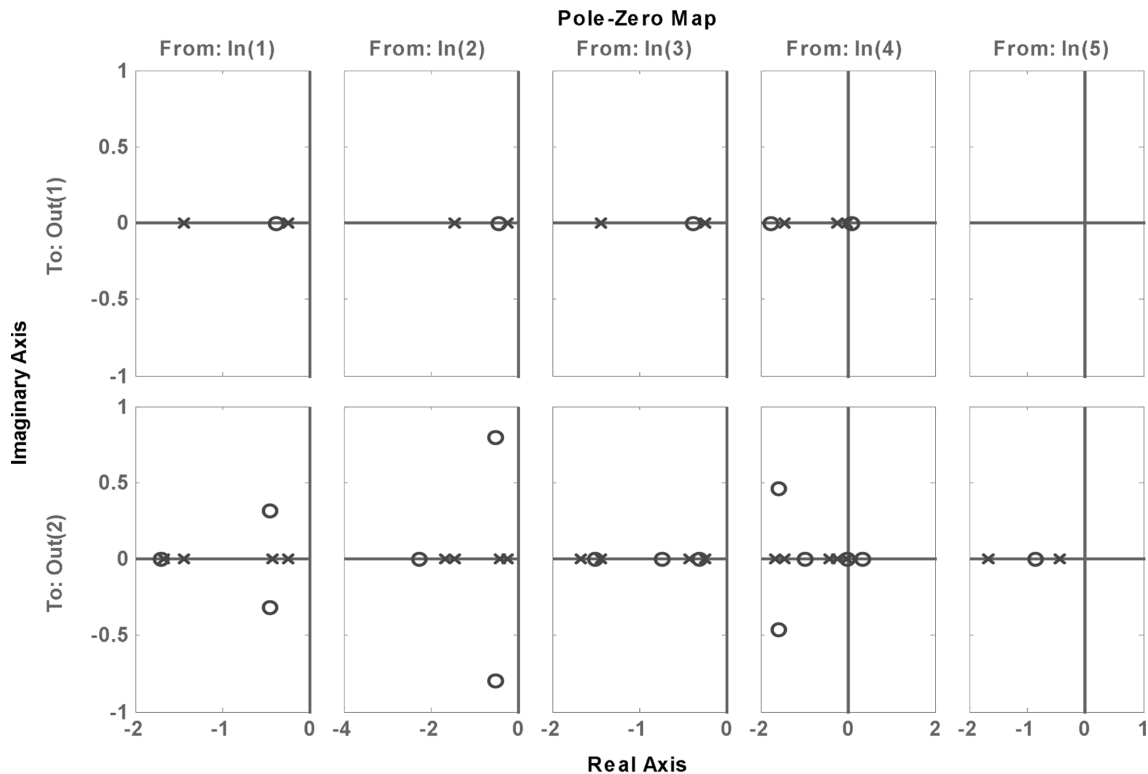

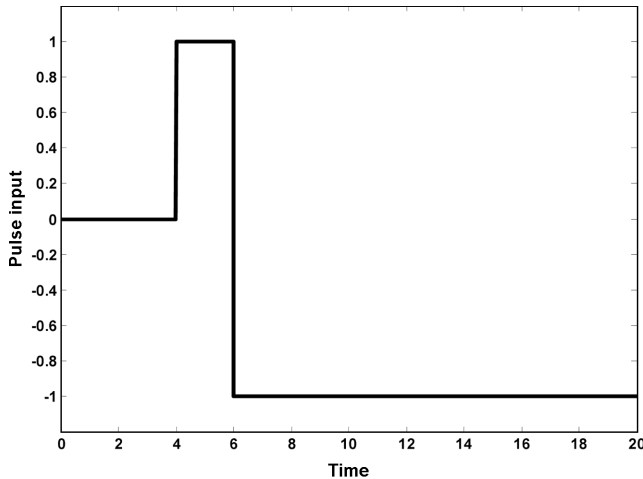**Fig. 2. Pole-zero map (x: pole, o: zero).**

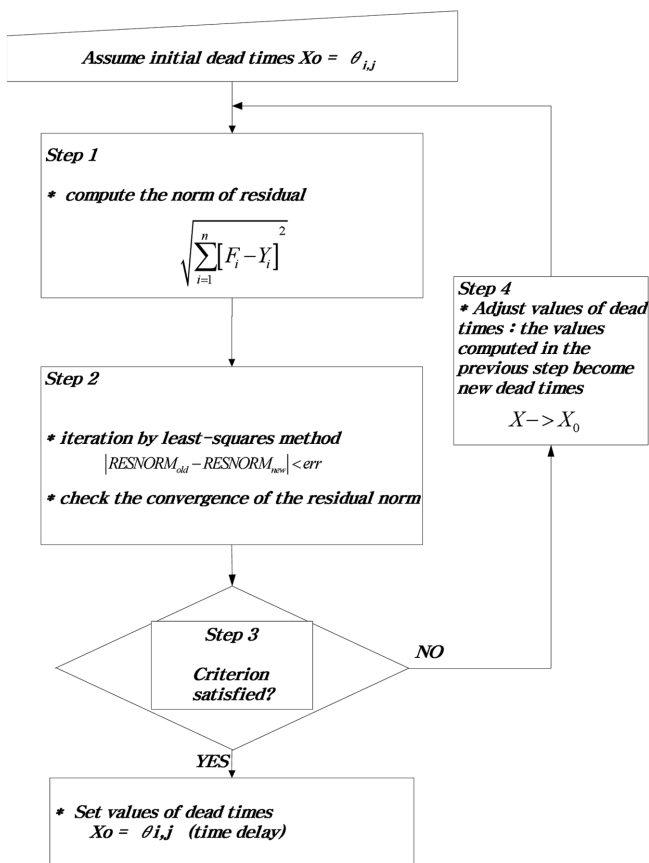Fig. 3. Pulse input used in the identification of lower-order models.

Fig. 4. Procedure for the determination of dead times.

for our purpose. Dead times contained in the models can easily be determined by using operational data. It is almost impossible to obtain exact values for the dead times. Fig. 4 shows the steps to determine dead times. First, initial values of dead times θ_{ij} are assumed

and iterative minimizations of residuals are followed to give optimal dead times. Resulting lower-order transfer functions can be expressed as (30) and results of corresponding dead time computations are given by (31).

$$\begin{pmatrix} Y1 \\ Y2 \end{pmatrix} = \begin{pmatrix} \dfrac{-0.05242 \cdot e^{-\theta_{11}}}{1.253s+1} & \dfrac{0.005675 \cdot e^{-\theta_{12}}}{1.572s+1} & \dfrac{0.07373 \cdot e^{-\theta_{13}}}{1.294s+1} \\[2mm] \dfrac{-0.01008 \cdot e^{-\theta_{21}}}{3.427s+1} & \dfrac{0.001334 \cdot e^{-\theta_{22}}}{14.23s+1} & \dfrac{0.05274 \cdot e^{-\theta_{23}}}{1.92s+1} \end{pmatrix}$$

$$\begin{pmatrix} \dfrac{(0.1322s+0.009898) \cdot e^{-\theta_{14}}}{13.82s^2+4.198s+1} & \dfrac{-1e\text{-}09 \cdot e^{-\theta_{15}}}{10s+1} \\[2mm] \dfrac{(0.1322s+0.009898) \cdot e^{-\theta_{24}}}{13.82s^2+4.198s+1} & \dfrac{35.53 \cdot e^{-\theta_{25}}}{1.608s+1} \end{pmatrix} \begin{pmatrix} U1 \\ U2 \\ U3 \\ U4 \\ U5 \end{pmatrix} \quad (30)$$

$$\theta_{min} = \begin{pmatrix} 0 & 1.3 & 0.3751 & 0.9865 & 1.3 \\ 0 & 1.3 & 0.3751 & 0.9865 & 1.3 \end{pmatrix} \quad (31)$$

NUMERICAL SIMULATIONS

Suitable initial values for the state variables C_s, X_s, C_2, X_{2a}, R and R_a should be assigned for the computations to be possible. Usually steady-state values for these variables are used as initial values. Table 1 shows initial values for the state variables used in the present work. Data sets obtained from the grade change operations were used to validate the simplified dynamic model. The first data set, being compared with the results of the simulation, was obtained during the change of the bone-dry weight (BD) from 66 g/m² to 56 g/m² (or from 70.8 g/m² to 61 g/m² in the basis weight (BW)).

Values of constants and parameters used in the simulations are shown in Table 2. In the model, rates of the thick stock flow, the retention aid and the filler inlet and the reel speed serve as input variables. Figs. 5 and 6 show changes of input variables used both in the actual plant operation and in the simulation. The ash fraction in the thick stock flow, X_{0a}, is dependent upon the extent of mixing of raw materials in the Broke and machine chest. X_{0a} exerts a strong influence on the ash content at the reel box, although BD is not affected by X_{0a}. The magnitude of X_{0a} is changed according to the paper grade. For this reason, the ash fraction should be considered as an input variable [Vhtamaki, 2001; Elkadiri and Berrada, 1997]. The ash fraction in the thick stock flow was assumed to exhibit the 2nd-order characteristics as given by

$$Y(s) = G(s) \cdot \frac{\Delta X_{0a}}{s} \qquad G(s) = \frac{1}{\tau_a^2 s^2 + 2\xi\tau s + 1} \quad (32)$$

where $\tau_a = 18$ and $\zeta = 1$ in the present study.

The same input variables were fed into the plant as well as the model. Results of the simulations are shown in Figs. 7, 8 and 9. Two key output variables (BD and ash BD) and four major state variables (consistencies in the silo and the headbox, the slurry rate and

Table 1. Initial state variables

State variables	C_s (kg/l or %/100)	X_{sa} (−)	C_2 (kg/l or %/100)	X_{2a} (−)	R (%)	R_a (%)
	0.009	0.235	0.0022	0.47	75	51

Table 2. Constants and parameters used in simulations

Description	
C_0 (kg/L) or (%/100)	0.0328
C_f (kg/L) or (%/100)	0.47
C_d (kg/L) or (%/100)	0.2
V (Liter)	105,000
V_s (Liter)	50,000
V_w (Liter)	1,000
V_{w1} (Liter)	2,000
k_1 (min/L)	0.0142
t (min)	800
P_w (Meter)	5.65
R_w (Meter)	4.06
C_w (Meter)	5.17
S_w (Meter)	0.01021
C_F (-)	0.92
J_r (-)	1.04
W_r (-)	0.85
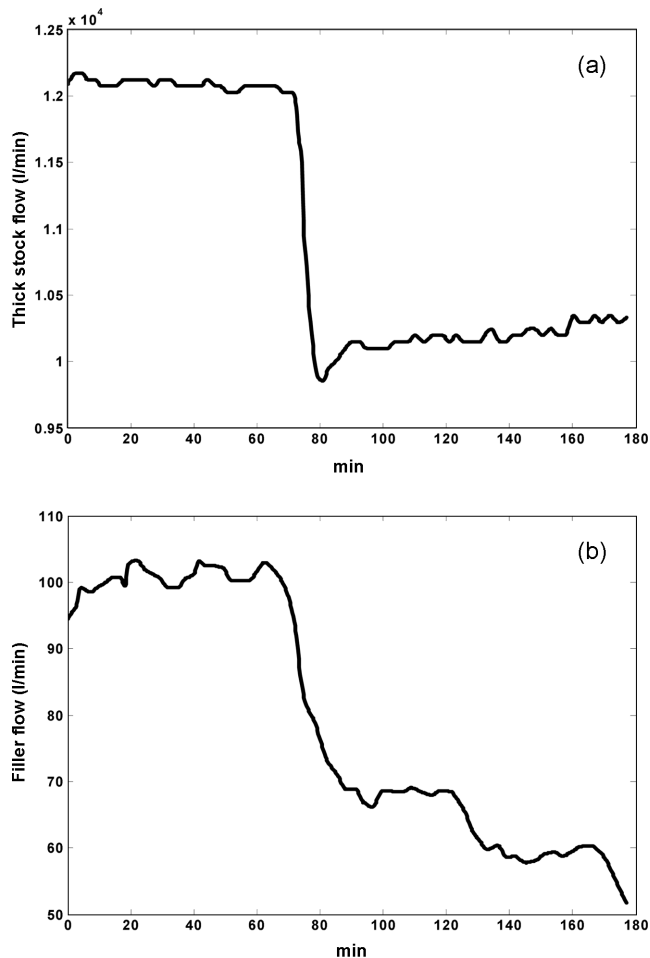
Fig. 5. Input flow rates of stock (a) and filler (b).

the retention ratio) were computed. Even with the up-to-date DCS technology, not all the variables are measured in the operation. In the plant being considered, BD and ash BD were detected online.
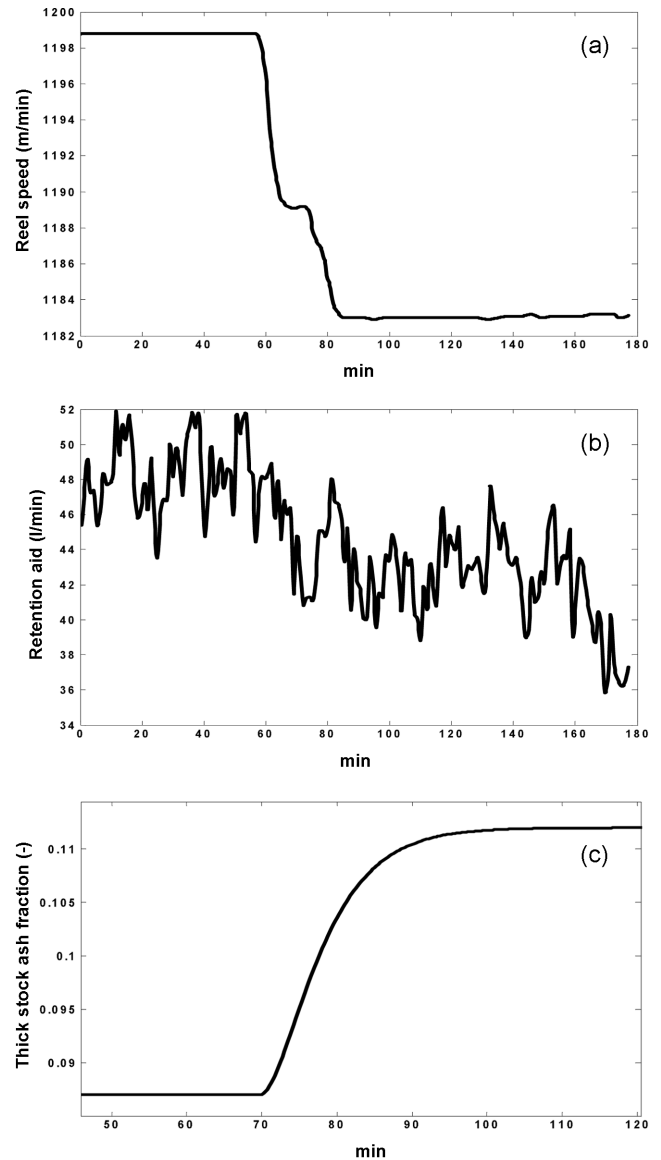
Fig. 6. Reel speed (a), flow rates of the retention aid (b), thick stock ash fraction (c).

We can see that the simplified model developed in the present study exhibits satisfactory tracking performance to the plant. The computed consistencies in the silo and the headbox shown in Fig. 8 display dynamic characteristics as expected. The smooth behavior of the silo consistency is not surprising considering the assumption of perfect mixing in the silo. Fig. 9 shows the slurry rate and the retention ratio obtained from the simulation. The retention ratio is another variable being detected online. The cause of the big discrepancy in the beginning is not clarified yet. But, without knowledge of the details of the detecting mechanism of the retention ratio, we can only say that the assumption of the perfect mixing in the silo might cause the discrepancy.

CONCLUSIONS

A dynamic model for the wet-end section of a paper mill was developed to characterize its dynamic behavior during the grade
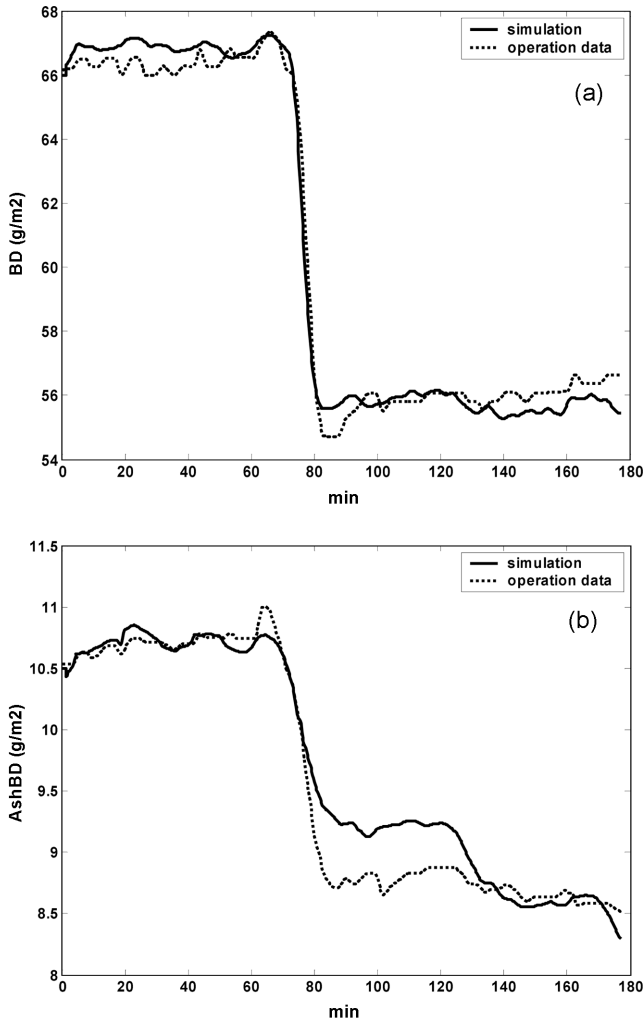
Fig. 7. Dynamics of bone-dry weight (a) and ash bone-dry weight (b).

Fig. 8. Dynamics of silo consistency (a) and headbox consistency (b).

change. The model is based on the mass balance relationships written for the simplified wet-end white water network. From the linearization of the dynamic model followed by Laplace transformation, higher-order transfer function models were obtained and stability of the models was examined. The 1st-order plus dead time (FOPDT) and 2nd-order plus dead time (SOPDT) models were identified based on the higher-order models by using least-squares method. Effects of key manipulated variables such as the thick stock flow, the filler flow and the retention aid flow on the major controlled variables were analyzed by numerical simulations. Results of simulations show a little discrepancy from the operational data, and we can see that the dynamics of the wet-end section of paper plants can be represented well by transfer functions with low-order plus dead times. The dynamic model developed in the present study in the form of Laplace transfer functions can be effectively used in the operation and control.

ACKNOWLEDGMENT

APPENDIX

$$A_{11}=(-p_1 \cdot V_r + 2 \cdot Q_0 + 2 \cdot Q_f + 2 \cdot Q_p + 2 \cdot V_w - p_2 \cdot V_r \cdot C_s \cdot R + V_{w1})/V$$
$$A_{21}=-((1-R_a) \cdot p_1 \cdot V_r \cdot C_s \cdot X_{sa} - p_1 \cdot V_r + p_2 \cdot V_r \cdot C_s \cdot R - V_{w1})/V/C_s^2$$
$$+X_{2a}/C_s^2 \cdot ((1-R) \cdot p_1 \cdot Reel \cdot C_s - (p_1 \cdot Vr - Q_0 - Q_f - Q_p - V_w) \cdot C_s$$
$$+(-p_2 \cdot Reel \cdot C_s \cdot R + V_{w1} + Q_0 + Q_f + Q_p + V_w) \cdot C_s)/V$$
$$-X_{2a}/C_s \cdot (-p_1 \cdot V_r + 2 \cdot Q_0 + 2 \cdot Q_f + 2 \cdot Q_p + 2 \cdot V_w - p_2 \cdot V_r \cdot C_s \cdot R + V_{w1})/V$$
$$A_{31}=(p_1 \cdot V_r - Q_0 - Q_f - Q_p - V_w)/V_s$$
$$A_{41}=(p_1 \cdot V_r - Q_0 - Q_f - Q_p - V_w) \cdot X_{2a}/V_s/C_s$$
$$-X_{sa}/C_s(p_1 \cdot V_r - Q_0 - Q_f - Q_p - V_w)/V_s$$
$$A_{51}=0$$
$$A_{61}=0$$

$$A_{12}=0$$
$$A_{22}=-1/C_s \cdot ((1-R) p_1 \cdot V_r \cdot C_s - p_1 \cdot V_r - Q_0 - Q_f - Q_p - V_w) \cdot C_s$$
$$+(-p_2 \cdot V_r \cdot C_s \cdot R + V_{w1} + Q_0 + Q_f + Q_p + V_w) \cdot C_s)/V$$

$$A_{32}=0$$
$$A_{42}=(p_1 \cdot V_r - Q_0 - Q_f - Q_p - V_w) \cdot C_s/V_s/C_s$$
$$A_{52}=0$$
$$A_{62}=0$$

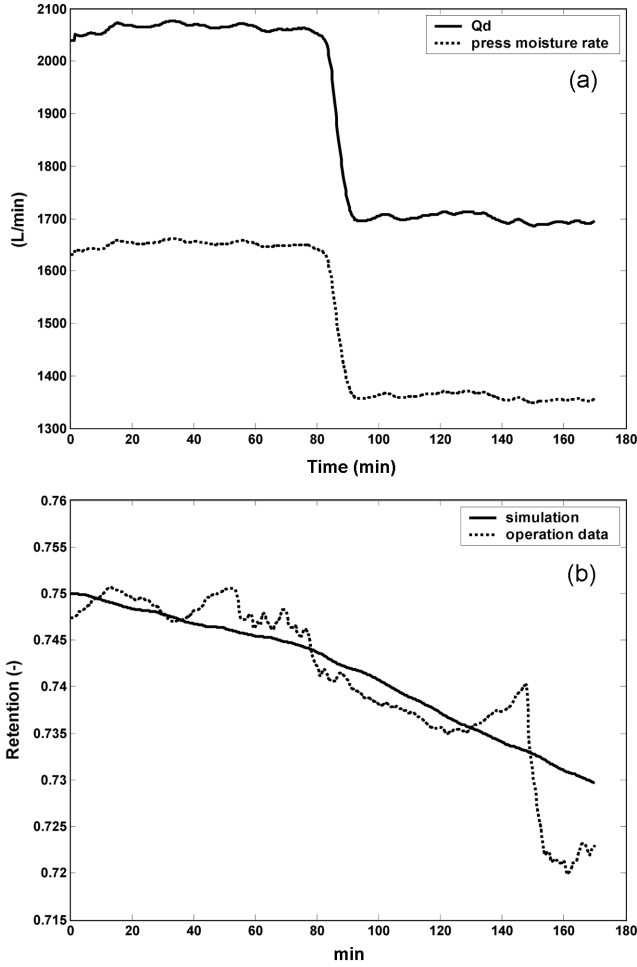**Fig. 9. Dynamics of slurry and moisture rates to the press (a) and retention ratio (b).**

$A_{13} = ((1-R) \, p_1 \cdot V_r - p_2 \cdot V_r \cdot R \cdot C_2)/V$

$A_{23} = ((1-R_a) \cdot p_1 \cdot V_r \cdot X_{sa} + p_2 \cdot V_r \cdot R)/V/C_s$
$\quad\quad - X_{2a}/C_s \cdot ((1-R) \cdot p_1 \cdot V_r - p_2 \cdot V_r \cdot R \cdot C_s)/V$

$A_{33} = -p_1 \cdot V_r/V_s$

$A_{43} = -(Q_0 \cdot C_0 \cdot X_{0a} + (p_1 \cdot V_r - Q_0 - Q_f - Q_p - V_w) \cdot C_2 \cdot X_{2a}$
$\quad\quad + Q_f \cdot C_f - p_1 \cdot V_r \cdot C_s \cdot X_{sa})/V_s/C_s^2 + X_{sa}/C_s^2 \cdot (Q_0 \cdot C_0$
$\quad\quad + (p_1 \cdot V_r - Q_0 - Q_f - Q_p - V_w) \cdot C_2 + Q_f \cdot C_f - p_1 \cdot V_r \cdot C_s)/V_s$

$A_{53} = 0$

$A_{63} = 0$

$A_{14} = 0$

$A_{24} = (1-R_a) \cdot p_1 \cdot V_r \cdot C_s/V/C_2$

$A_{34} = 0$

$A_{44} = -p_1 \cdot V_r/V_s - 1/C_s \cdot (Q_0 \cdot C_0$
$\quad\quad + (p_1 \cdot V_r - Q_0 - Q_f - Q_p - V_w) \cdot C_2 + Q_f \cdot C_f - p_1 \cdot V_r \cdot C_s)/V_s$

$A_{54} = 0$

$A_{64} = 0$

$A_{15} = (-p_1 \cdot V_r \cdot C_s - p_2 \cdot V_r \cdot C_s \cdot C_2)/V$

$A_{25} = p_2 \cdot V_r \cdot C_s/V/C_2 - X_{2a}/C_2 \cdot (-p_1 \cdot V_r \cdot C_s - p_2 \cdot V_r \cdot C_s \cdot C_2)/V$

$A_{35} = 0$

$A_{45} = 0$

$A_{55} = -1/\tau$

$A_{65} = 0$

$A_{16} = 0$

$A_{26} = -p_1 \cdot V_r \cdot C_s \cdot X_{sa}/V/C_2$

$A_{36} = 0$

$A_{46} = 0$

$A_{56} = 0$

$A_{66} = -1/\tau$

$B_{11} = ((1-R) \cdot p_1 \cdot C_s - p_1 \cdot C_2 - p_2 \cdot C_s \cdot R \cdot C_2)/V$

$B_{21} = ((1-R_a) \cdot p_1 \cdot C_s \cdot X_{sa} - p_1 + p_2 \cdot C_s \cdot R)/V/C_2$
$\quad\quad - X_{2a}/C_2 \cdot ((1-R) \cdot p_1 \cdot C_s - p_1 \cdot C_2 - p_2 \cdot C_s \cdot R \cdot C_2)/V$

$B_{31} = (p_1 \cdot C_2 - p_1 \cdot C_s)/V_s$

$B_{41} = (p_1 \cdot C_2 \cdot X_{2a} - p_1 \cdot C_s \cdot X_{sa})/V_s/C_s - X_{sa}/C_s \cdot (p_1 \cdot C_2 - p_1 \cdot C_s)/V_s$

$B_{51} = 0$

$B_{61} = 0$

$B_{12} = 2 \cdot C_2/V$

$B_{22} = -2 \cdot X_{2a}/V$

$B_{32} = (C_0 - C_2)/V_s$

$B_{42} = (C_0 \cdot X_{0a} - C_2 \cdot X_{2a})/V_s/C_s - X_{sa}/C_s \cdot (C_0 - C_2)/V_s$

$B_{52} = 0$

$B_{62} = 0$

$B_{13} = 2 \cdot C_2/V$

$B_{23} = -2 \cdot X_{2a}/V$

$B_{33} = (-C_2 + C_f)/V_s$

$B_{43} = (-C_2 \cdot X_{2a} + C_f)/V_s/C_s - X_{sa}/C_s \cdot (-C_2 + C_f)/V_s$

$B_{53} = 0$

$B_{63} = 0$

$B_{14} = 2 \cdot C_2/V$

$B_{24} = -2 \cdot X_{2a}/V$

$B_{34} = -C_2/V_s$

$B_{44} = -C_2 \cdot X_{2a}/V_s/C_s + X_{sa}/C_s \cdot C_2/V_s$

$B_{54} = k_1/\tau$

$B_{64} = k_2/\tau$

$B_{15} = 0$

$B_{25} = 0$

$B_{35} = 0$

$B_{45} = Q_0 \cdot C_0/V_s/C_s$

$B_{55} = 0$

$B_{65} = 0$

$$C = \begin{pmatrix} 0 & 0 & p_1 p_3 R & 0 & p_1 p_3 C_s & 0 \\ 0 & 0 & p_1 p_3 X_{sa} R_a & p_1 p_3 C_s R_a & 0 & p_1 p_3 C_s X_{sa} \end{pmatrix}$$

D = zero matrix

NOMENCLATURE

ashBD : bone-dry basis weight of ash [g/m²]

BD : bone-dry basis weight [g/m²]

C_0 : consistency in the thick stock [kg/L or %/100]

C_2 : consistency in the silo [kg/L or %/100]

C_d : consistency to press [kg/L or %/100]
C_f : consistency in the filler flow [kg/L or %/100]
C_F : headbox slice factor [-]
C_s : consistency in the headbox [kg/L or %/100]
C_w : the width of the couch [m]
J_r : jet/wire ratio [-]
k : draw factor [-]
k_1 : retention constant [min/L]
k_2 : ash retention constant [min/L]
Q_0 : thick stock flow rate [L/min]
Q_2 : internal recirculation flow rate [L/min]
Q_d : flow rate to the press [L/min]
Q_f : ash flow rate [L/min]
Q_p : flow rate of the retention aid [L/min]
Q_{pdf} : flow rate to saveall [L/min]
Q_s : outlet flow rate from the headbox [L/min]
Q_T : flow rate in the tray [L/min]
R : retention ratio [-]
R_a : ash retention ratio [-]
P_w : width of the pond [m]
R_w : the width of the reel [m]
S_w : the gap of the slice [m]
V : silo volume [L]
V_r : reel speed [m/min]
V_s : stock approach volume [L]
V_w : the amount of dilution water [L/min]
V_{w1} : clean water rate to the silo [L/min]
W_r : diminishment ratio [-]
X_{0a} : ash fraction in the thick stock [-]
X_{2a} : ash fraction in the silo [-]
X_{sa} : ash fraction in the headbox [-]

Greek Letters

τ : retention time constant [min]
τ_a : 2nd order transfer function time constant [min]
θ_{ij} : dead times [min]
ζ : 2nd order transfer function damping factor [-]

REFERENCES

Berrada, M. E., Tarasiewicz, S., Elkadiri, M. E. and Radziszewski, P. H., "A State Model for the Drying Paper in the Paper Product Industry," *IEEE Transactions on Industrial Electronics*, **44**(4), 579 (1997).

Chyi, H. and Chuang, Y., "Computation of Optimal Reduced-order Models with Time Delay," *Chem. Eng. Sci.*, **49**(19), 3291 (1994).

Elkadiri, M. E. and Berrada, M. E., "The Wet-end in Pulp and Paper Industry: Controllers and Simulation Results," Record of Annual Pulp and Paper Industry Technical Conf., IEEE, Cincinnati., 97 (1997).

Hauge, T. A. and Lie, B., "Paper Machine Modeling at Norske Skog Saugbugs: A Mechanistic Approach," *Modeling, Identification and Control*, **23**(1), 27 (2002).

Mardon, J., Jackson, M. and Serenius, R., "The Theory and Application of the Wet end Materials Balance," *Appita J.*, **25**(1), 45 (1971).

Murphy, T. F. and Chen, S. C., "Transition Control of Paper-making Processes: Paper Grade Change," Proc. IEEE intl. Conf. on control Applications, IEEE, Hawaii, 1278 (1999).

Neimo, L., *Papermaking Science and Technology: Paper Making Chemistry (Book 4)*, Ch. 4, Tappi press, Helsinki (2000).

Norman, B., "The Water and Fiber Flow System in the Paper and Board Mill," Print Paper and Board Products for Printing in the Nineties Conf. Proc., EUCEPA, Paris, 217 (1990).

Skoglund, A. and Brundin, A., "A Multivariate Process Model for Grade Change in a Paperboard Machine," *Nordic Pulp and Paper Res. J.*, **15**(3), 183 (2000).

Vhtamaki, P., "Hybrid Modeling of Moisture in Paper Machine Grade Changes," *Pulp Paper Can*, **102**(7), 30 (2001).

Yeo, Y. K., Roh, H. D., Kim, I. W., Moon, I. and Chung, Y., "Optimal Operation of Utility Systems in Petrochemical Plants," *Korean J. Chem. Eng.*, **20**, 200 (2003).

Yeo, Y. K., Yi, S. C., Ryu, J. Y. and Kang, H., "Modeling and Simulation of Wet-end White Water System in the Paper Mill," *Korean J. Chem. Eng.*, **21**, 358 (2004).